Theor Chem Account (2008) 120:363–374
DOI 10.1007/s00214-008-0411-1

REGULAR ARTICLE

Quantitative derivation of the bijective link between molecular data and UV–visible absorption spectra for diluted molecules: guidelines for non specialists

Rémy Fortrie · Henry Chermette

Received: 25 August 2007 / Accepted: 31 January 2008 / Published online: 7 March 2008

Abstract In this article, we give a detailed derivation of the theoretical sequence leading from molecular data to UV–visible absorption spectra, and back from absorption spectra to molecular data, in the widely encountered case of linearly absorbent molecular species homogeneously and isotropically diluted in a homogeneous and isotropic transparent matrix or solvent. At each step of the derivation, assumptions and approximations are clearly explained and references are provided for the justifications which are out of the scope of the present article. The precision and the limitations of such spectroscopic investigations are then underlined and quantified on two examples: a hypothetic academic one-dimensional system and the $Ni(H_2O)_6^{2+}$ aqueous complex. The present interdisciplinary article aims to contribute to more efficient, and more and more necessary, interplays and mutual interactions between theoreticians and experimentalists by providing, to nonspecialists of both sides, a rather complete but clear and accessible description of the previously mentioned bijective sequence.

Keywords Spectroscopy · UV–visible · Absorption · Theory · Experiment · Quantitative · Link

1 Introduction

In a previous paper [13], we defined a new tool for the quantification of two-photon absorption, the two-photon absorption strength, and we also explained how its values can be quantitatively extracted from experimental data. In a more recent paper [15], we practically used it to quantify the enhancement of two-photon absorption observed in fluorene oligomers. Analyzing this enhancement, however, also requires the quantitative extraction of one-photon absorption properties from experimental UV–visible absorption spectra. We were however, and to our greatest surprise, unable to find, among the literature to which we had access, and which represents several tenners of physical chemistry books and a huge quantity of research articles, any equivalent of the derivation we had performed for two-photon absorption but in the case of one-photon absorption.

This is particularly astonishing, since the measurement of one-photon absorption spectra [34] is nowadays an extensively used technique for investigating the electronic properties of materials. It has indeed been successfully applied to gas phase molecules [20], organic compounds [41], complexes [31], polymers [24], clusters [29], biomolecules [5], matrix isolated species [3], surfaces [10] and solids [26]. As a consequence of its success, this technique has now been taught for many years from the A level to the Master's Degree and hundreds of physical chemistry textbooks exist that deal with this topic. Most of these books exhibit both a theoretical and an experimental section which are fully detailed. However, to our greatest disappointment, the description of the quantitative link between these two descriptions of the

This paper is dedicated to the 60th birthday of Nino Russo.

R. Fortrie
Université de Lyon,
École Normale Supérieure de Lyon,
CNRS UMR 5182, Laboratoire de Chimie, 46 Allée d'Italie,
69364 Lyon Cedex 07, France

H. Chermette (✉)
Université de Lyon, Université Lyon 1,
CNRS UMR 5180 Sciences Analytiques,
Chimie Physique Théorique, Bât. Paul Dirac (210),
43 Boulevard du 11 Novembre 1918,
69622 Villeurbanne Cedex, France
e-mail: Henry.Chermette@univ-lyon1.fr

same phenomenon is most often very limited. For UV–visible absorption spectra of diluted species for example, which is precisely the case we are here interested in, and which is rather often encountered in every-day life, the formulae used for extracting molecular data (transition energies and transition electric dipole moments) from experimental absorption spectra are generally given with no justification (see for example [21]).

On the contrary of our previous papers, the present article is exclusively dedicated to one-photon absorption spectra. It aims to fill the previously described lack by providing a clear and accessible derivation of the relations that allow the extraction of electronic molecular data from UV–visible absorption spectra in the particular case of molecular species homogeneously and isotropically diluted in a homogeneous and isotropic transparent matrix or solvent. As the reader will observe, this link is less obvious than it could first appear.

This article aims to contribute to a more efficient collaboration between theoreticians and experimentalists by making the previously mentioned derivation accessible to nonspecialists of both sides, which means theoreticians who are usually not involved in spectroscopic problems and spectroscopist, or more generally physicists and chemists, who are not so used to theoretical chemistry. It is then written in such a way that all previously described target readers can easily understand it, and, as a consequence, information and equations are reported in this paper that may appear obvious for some of the readers. A special effort is however, achieved to maintain it as compact as possible, and also to avoid excessive simplifications which could lead to a deformed view of the state of the art.

This paper is organized as follows. First, the theoretical sequence leading from molecular data to UV–visible absorption spectra is presented. Second, the reverse procedure is detailed and the methods usually used for the extraction of electronic molecular data from UV–visible absorption spectra are explained. At each step of the derivation, assumptions and approximations are highlighted, as well as their limitations and consequences. Third, these last points are illustrated thanks to two typical examples: first an hypothetic academic one-dimensional system and then the $Ni(H_2O)_6^{2+}$ aqueous complex.

2 From molecular to experimental data

All numerical objects are here given in standard international units [30].

2.1 Absorption coefficient and refractive index

All derivations reported in this article concern, in the absence of other mention, a single diluted absorbent molecular entity. However, on account on the linearity of all subsequent relations, the generalization to the case of a mixture of diluted absorbent molecular entities is straightforward. The total absorbance of the mixture (see below) is indeed equal to the sum of the absorbance of all individual species.

From a general point of view, the equation that links the electric field and the polarization within a nonmagnetic dielectric medium is (1), where $\mathbf{e}_\omega$ and $\mathbf{p}_\omega$ represent the ω-frequency Fourier components of the time- and space-dependent electric field and polarization respectively, c the speed of light and ε_0 the vacuum permitivity [12].

$$\Delta\mathbf{e}_\omega + \frac{\omega^2}{c^2}\mathbf{e}_\omega - \nabla\left(\nabla\cdot\mathbf{e}_\omega\right) = -\frac{\omega^2}{\varepsilon_0 c^2}\mathbf{p}_\omega \tag{1}$$

As previously mentioned, we are here only concerned with linear, homogeneous and isotropic media. Relation (1) then simplifies into relation (2), where χ_ω is a complex number and represents the frequency dependent mesoscopic average linear polarizability of the medium.

$$\Delta\mathbf{e}_\omega + \frac{\omega^2}{c^2}\left(1+\frac{\chi_\omega}{\varepsilon_0}\right)\mathbf{e}_\omega = 0 \tag{2}$$

A sample is now considered that consists of a single linearly absorbent molecular species homogeneously and isotropically diluted in a homogeneous and isotropic transparent matrix, which is a particular case of linear, homogeneous and isotropic nonmagnetic dielectric medium. The molecular concentration of the diluted compound is hereafter noted N. This sample is assumed crossed by a planar and monochromatic electromagnetic wave with frequency ω, whose mathematical expression is $\mathbf{a}_\omega \exp\left(ik_\omega \mathbf{u}_\omega\cdot\mathbf{r}\right)$, which is a particular solution of Eq. (2). In this last expression, $\mathbf{a}_\omega$ is the polarization vector (not to be confused with the polarization of the medium) and $k_\omega\mathbf{u}_\omega$ is the wave vector, where $\mathbf{u}_\omega$ is a real unitary vector of space and k_ω a complex number, such that relation (3) is verified.

$$k_\omega^2 = \frac{\omega^2}{c^2}\left(1+\frac{\chi_\omega}{\varepsilon_0}\right) \tag{3}$$

The light beam is here assumed being a plane wave, but real light beams are of course not. Measured intensities of real light beams are obtained through the integration of their local intensities over their whole sections. However, because of the linearity of Eq. (2), this does not make any difference in the following treatment, which can be extended to any shape of light beam.

A sample slice is now considered, whose characteristic planes are assumed orthogonal to $\mathbf{u}_\omega$ and whose thickness is noted L. The absorbance A_ω of this slice is then defined by relation (4), where $I_\omega(\mathbf{0})$ represents the average incoming light beam intensity and $I_\omega(L\mathbf{u})$ the average transmitted light beam intensity.

$$A_\omega = \log_{10}\left(\frac{I_\omega(\mathbf{0})}{I_\omega(L\mathbf{u})}\right) \tag{4}$$

Within the restrictive framework of this study, the expression of the previously mentioned intensity, which is defined by relation (5), is obtained by relation (6), where $\Re$ and $\Im$ represent the real part and imaginary part operators, respectively, which leads to expression (7) for the absorbance of the sample.

$$I_\omega = \frac{\varepsilon_0 c^2}{2\omega} \Im\left[(\mathbf{e}_\omega)^* \times (\nabla \times \mathbf{e}_\omega)\right] \tag{5}$$

$$I_\omega(\mathbf{r}) = \frac{\varepsilon_0 c^2 |\mathbf{a}_\omega|^2 \Re(k_\omega)}{2\omega} \exp\left[-2\Im(k_\omega)\, \mathbf{u}_\omega \cdot \mathbf{r}\right] \tag{6}$$

$$A = \frac{2L\Im(k)}{\log_e(10)} \tag{7}$$

The absorption coefficient of the molecular entity of interest at frequency ω, ε_ω, is, by definition, equal to AN_A/NL, where N_A is Avogadro's number, and verifies then here relation (8) [30].

$$\varepsilon_\omega = \frac{2N_A\Im(k_\omega)}{N\log_e(10)} \tag{8}$$

For weakly absorbent media, which is a case quite frequently encountered in every day life UV–visible absorption spectra measurements,[1] and which is mathematically characterized by the fact that $\Im(k_\omega)$ is negligible with respect to $\Re(k_\omega)$, relation (3) can be expressed as a limited development with respect to $\Im(\chi_\omega)/\Re(\chi_\omega)$ and relation (8) can be converted into relation (9), where n_ω is the refractive index of the medium and is related to its polarizability through relation (10).

$$\varepsilon_\omega = \frac{\omega N_A \Im(\chi_\omega)}{N\varepsilon_0 c n_\omega \log_e(10)} \tag{9}$$

$$n_\omega = \sqrt{1 + \frac{\Re(\chi_\omega)}{\varepsilon_0}} \tag{10}$$

2.2 Molecular polarizability

Within the previous section, no mention has been done of the molecular properties of the absorbent species. The absorption coefficient of the medium, which is an experimentally accessible data, has indeed only been linked to the average mesoscopic polarizability of the medium at frequency ω. In this section, we now focus on the frequency dependent molecular polarizability of the molecular entity of interest.

From a quantum mechanical point of view, a molecular entity is characterized by its quantum eigenstates,[2] which are here represented by $|m\rangle$, where m is an integer number and where $|0\rangle$ represents the ground state of the system. At this point of the derivation, no assumption is done about the rovibronic nature of these eigenstates. Each one of these states is associated to an energy E_m and to an energetic width Γ_m which depends on the life-time τ_m of the state of interest through Eq. (11), where $\hbar$ represents the reduced Planck's constant.

$$\Gamma_m = \frac{\hbar}{\tau_m} \tag{11}$$

As for a macroscopic system, the polarization of a molecular entity depends on the electric field applied. As previously mentioned, only molecules exhibiting linear responses are here considered (see reference [13] and references therein for nonlinear responses). Within this framework, each Fourier component π_ω of the molecular polarization linearly depends on the Fourier component $\mathbf{e}_\omega$ of the applied electric field through relation (12), where $\hat{\alpha}(\omega)$ is the first molecular polarizability tensor.

$$\pi_\omega = \hat{\alpha}(\omega) \cdot \mathbf{e}_\omega \tag{12}$$

It can then be shown, using the time-dependent perturbation theory [33], which is out of the scope of this paper, that the matrix elements of $\hat{\alpha}(\omega)$ depend on energies E_m, on widths Γ_m and on the transition electric dipole moments $\langle m|\mu|n\rangle$ between the eigenstates of the molecular system through relation (13), where q represents the current state of the molecular system, i and j take their values among the cartesian directions x, y and z, and where Ω_{qm} is defined by relations (14) and (15).

$$\alpha_{i,j}(\omega) = \frac{1}{\hbar}\sum_{m\neq q}\left\{\frac{\langle q|\mu_i|m\rangle\langle m|\mu_j|q\rangle}{\Omega_{qm}-\omega} + \frac{\langle q|\mu_j|m\rangle\langle m|\mu_i|q\rangle}{\Omega_{qm}^*+\omega}\right\} \tag{13}$$

$$\Omega_m = \frac{1}{\hbar}\left(E_m - i\frac{\Gamma_m}{2}\right) \tag{14}$$

$$\Omega_{qm} = \Gamma_m - \Gamma_q \tag{15}$$

E_m, Γ_m and $\langle m|\mu|n\rangle$ are theoretical data that can be estimated using, for example, computational chemistry programs, and molecular polarizabilities are then theoretically accessible via relation (13). The next step of this study then of course consists in describing the link between mesoscopic polarizability and molecular polarizability.

[1] The maximum measurable absorbance for usual spectrophotometer is indeed around 3 and the tightest usable sample cell about 1-μm thin, which makes the maximum value of $\mathrm{Im}(k)$ equal to 3.45×10^6 smallest refraction index of usual samples is equal to 1 and the longest wave length accessible with usual UV–visible spectrophotometers is 2,000 nm, which makes the smallest value of $\mathrm{Re}(k)$ equal to 3.14×10^6 m^{-1}. It can then be seen that all extreme experimental conditions have to be met at the same time for $\mathrm{Im}(k)$ and $\mathrm{Re}(k)$ being of the same magnitude. For more usual cases, like a 10 mm tight sample cell and an absorbance of 1, the ratio $\mathrm{Im}(k)/\mathrm{Re}(k)$ falls down to 3.66×10^{-5}, which is, as a matter of fact, negligible with respect to 1.

[2] Dirac notations are used in this article. Their definitions and properties are detailed in most quantum mechanics textbooks.

2.3 Local field approximation

First must be decided which molecular entity has to be considered. Indeed, on the contrary of gas phase molecular entities, which are spatially well separated and then rather well defined,[3] each molecular entity of interest is here surrounded by a quite large number of other solvent or matrix molecular entities whose presence directly influences the rotational, vibrational and electronic properties of the molecular entity of interest itself. The way the molecular entity has however, to be chosen is unfortunately as unprecise as the definition of a molecular entity itself [30].

The way the surrounding molecular entities are taken into account strongly depends on the nature of both the molecular entity of interest and the solvent or the matrix. For metallic cations diluted in water, for example, well-organized complexes appear that have to be treated as molecular entities [23]. On the contrary, for ketones species diluted in alkane species, for example, the interaction between the molecular entity of interest and the solvent is rather weak [40] and the influence of the solvent on the electronic properties of the ketone can be rendered by an average effect, since no structural order appears.

An explicit and quantitative link between, on one hand, molecular theoretically accessible data and, on the other hand, macroscopic experimentally accessible data is mainly required in two cases: for validating theoretical simulations, and for extracting molecular data from experimental data.

Concerning the validation of theoretical simulations, however, a notable exception exists. Computational simulations can indeed be performed using two different strategies: the periodic approach and the cluster approach.[4] The first method consists in explicitly simulating a set of solvent molecules and absorbent molecules gathered in a finite cell which is periodically replicated by translation an infinite number of time to fill the complete space [38]. In such a case, the mesoscopic polarizability of the medium is directly accessible.[5] Within the framework of the cluster approach, however, which consists in modeling the properties of a unique spatially limited molecular entity, and which is to our knowledge, at the moment, the most extensively used while modeling molecular properties, the calculated molecular polarizability has to be converted to a mesoscopic polarizability for achieving comparison with experiment.

One extensively used method for quantitatively linking molecular and mesoscopic polarizabilities is the so called *local field approximation* [9,28]. It is assumed that the molecular entity of interest is located in a spherical empty cavity buried within the solvent or the matrix, this last being considered continuous. It is then shown that the frequency-dependent electric field $\mathbf{e}_{\omega}^{(\mathrm{loc})}$ felt by the molecular entity located in the cavity depends on the external (mesoscopic) applied frequency-dependent electric field $\mathbf{e}_{\omega}$ via relation (16).

$$\mathbf{e}_{\omega}^{(\mathrm{loc})} = \mathbf{e}_{\omega} + \frac{1}{3\varepsilon_0}\mathbf{p}_{\omega} \tag{16}$$

From a general point of view, molecules tend to adapt their orientation to the applied electric field. Taking this phenomenon into account has been achieved by Onsager [32]. The importance of this reorientation however, strongly depends on the frequency of the applied electromagnetic field, and is, in particular, rather small in the UV–visible range. It will then not be considered further in this article.

2.4 Lorentz factors

The mesoscopic polarization of a material is, by definition, equal to the sum of the molecular polarizations of all molecular entities contained in the material. As a direct consequence, for a homogeneous material consisting in a mixture of B molecular species indiced with b, relation (17) is verified, where N_b represents the molecular quantity of species b and $\mathbf{p}_{\omega}^{(b)}$ the average mesoscopic polarizability due to b type molecular entities.

$$\mathbf{p}_{\omega} = \sum_{b=1}^{B} N_b \mathbf{p}_{\omega}^{(b)} \tag{17}$$

From relation (17), using relations (16) and (12), and assuming an isotropic material, it is shown that relation (18) is verified, where the (b) exponent is added to the previously used notations to specify that a data refers to a the molecular species b, and where $\bar{\alpha}_{\omega}^{(b)}$ is defined by relation (19). L_{ω} is called *Lorentz factor* and is defined by relation (20).

$$\bar{\chi}_{\omega}^{(b)} = L_{\omega}\bar{\alpha}_{\omega}^{(b)} \tag{18}$$

$$\bar{\alpha}_{\omega}^{(b)} = \frac{1}{3}\left[\alpha_{xx}^{(b)}(\omega) + \alpha_{yy}^{(b)}(\omega) + \alpha_{zz}^{(b)}(\omega)\right] \tag{19}$$

$$L_{\omega} = \frac{1}{1 - \frac{1}{3\varepsilon_0}\sum_{b=1}^{B} N_b \bar{\alpha}_{\omega}^{(b)}} \tag{20}$$

If the dilution is high enough, the difference between the contribution of the diluted molecular entities and the contribution of the solvent is negligible with respect to the contribution of the solvent. As a consequence, for sufficiently diluted molecular entities, it is shown, using a limited development, that relations (21) and (22) are verified, where n_S

[3] Note that this may not be the case any more for gas phases under high pressures or for systems exhibiting exiplexes or eximers.

[4] Actually, hybrid methods also exist that combine both approaches [37].

[5] Depending on the number of absorbent molecules per cell, averaging the calculated mesoscopic polarizability tensor over all directions of space may be required.

represents the refractive index of the solvent. [6]

$$\Im(\chi_\omega) = L_\omega^2 \sum_{b=1}^{B} N_b \Im\left(\bar{\alpha}_\omega^{(b)}\right) \tag{21}$$

$$L_\omega = \frac{n_S^2 + 2}{3} \tag{22}$$

In relation (21), the presence of the Lorentz factor at the power 2 may look surprising considering relations (17), (18) and (22). It however, simply comes out from the fact that L_ω, before being approximated, also depends on $\bar{\alpha}_\omega^{(b)}$, which has to be taken into account while performing the previously mentioned limited development, which gives rise to relation (21).

2.5 Absorption coefficient

It then comes out, using relations (9) and (18), that, within the framework of a single absorbent molecular species, the absorption coefficient depends on the molecular polarizability of the absorbent molecular entity through relation (23), where $\bar{\alpha}_\omega$ now refer to the only absorbing molecular species contained by the material.

$$\varepsilon_\omega = \left(\frac{n_S^2 + 2}{3}\right)^2 \frac{\omega N_A \Im(\bar{\alpha}_\omega)}{\varepsilon_0 c n_S \log_e(10)} \tag{23}$$

Finally, using relations (13) and (19), we end up with expression (24), where g_q represents the fraction of absorbent molecular entities in state $|q\rangle$.

$$\varepsilon_\omega = \left(\frac{n_S^2 + 2}{3}\right)^2 \frac{N_A \omega}{3\hbar\varepsilon_0 c n_S \log_e(10)} \times \sum_{q=0}^{+\infty} g_q \sum_{m=1}^{+\infty} \frac{\Gamma_m}{2} \frac{\mu_{qm}^2}{(\omega_{qm} - \omega)^2 + \frac{\Gamma_m^2}{4}} \tag{24}$$

2.6 Oscillator strength

Relation (24) may be transformed using oscillator strengths f_{qm}, which is a pure theoretical object, whose definition is given by relation (25) [7]. In that relation, m_e represents the electron mass and e the elementary charge.

$$f_{qm} = \frac{2m_e}{3e^2\hbar} \omega_{qm} \mu_{qm}^2 \tag{25}$$

[6] Refractive indices of solvents, as well as those of the cells used for UV–visible absorption spectra measurements, generally depend on the frequency associated to the electromagnetic radiation. They can however, usually be assumed constant over a wide range of frequencies without significant lost of precision. The extreme values of the corresponding frequency window depend of course on the chosen solvent or cell and have to be checked before interpreting measurements [1,16].

Oscillator strengths are used while describing atomic spectra [7] and are also extensively used by theoretical chemistry computational codes [27]. Indeed, from a practical point of view, oscillator strengths do not bear any unit and take values around unity for spin- and spatially-authorized electronic transitions in small molecules.

A particularity of oscillator strengths is that, for any molecular entity containing N electrons, they fulfill the Thomas–Reiche–Kuhn sum rule (26) [18,25,35,39].

$$\sum_m f_{qm} = N \tag{26}$$

Since relation (24) explicitly links molecular data (transition energies and transition electric dipole moments) to experimental data (absorption coefficient) it should a priori be possible to extract molecular data from UV–visible absorption spectra. This is the topic of the next section.

3 From UV–visible absorption spectra to molecular data

3.1 Hypothetic set of isotropically and homogeneously distributed akinetic isolated molecules

For isolated molecules, energetic widths Γ_m are generally small if compared to energy differences between rovibronic eigenstates [4]. As a consequence, UV–visible absorption spectra of hypothetic sets of homogeneously and isotropically spread akinetic isolated molecular entities consist in sets of ideally well separated rays, each corresponding to a single rovibronic transition of the molecular entity of interest. In such a particular case, rays are fitable using Eq. (24) and parameters Γ_m, ω_{qm} and μ_{qm} $(= |\mu_{qm}|)$ are directly accessible. Is is however, also true that ω_{qm} parameters are equal to the frequencies that correspond to maxima of ε_ω, and that μ_{qm} parameters are obtained using one of both integrative methods represented by relations (27) and (28), where $\int_{\omega_{qm}}$ means that the integration is restricted to the single ray located at ω_{qm}.

$$\int_{\omega_{qm}} \frac{\varepsilon_\omega}{\omega} \mathrm{d}\omega = \frac{N_A \pi}{3\hbar c \varepsilon_0 n \log_e(10)} \left(\frac{n^2 + 2}{3}\right)^2 g_q \mu_{qm}^2 \tag{27}$$

$$\frac{1}{\omega_{qm}} \int_{\omega_{qm}} \varepsilon \mathrm{d}\omega = \frac{N_A \pi}{3\hbar c \varepsilon_0 n \log_e(10)} \left(\frac{n^2 + 2}{3}\right)^2 g_q \mu_{qm}^2 \tag{28}$$

Both expressions directly result from the integration of $\varepsilon_\omega/\omega$ and ε_ω respectively using relation (24). On the contrary of what could be first thought looking at relations (27) and (28), relation (28) is *not* an approximation of relation (27). Both are indeed mathematically exact and use the only assumption that the ray of interest is perfectly isolated. From

a practical point of view, however, relation (27) presents the advantage that the integral can be evaluated over frequencies or wave lengths—both commonly used unit scales for representing absorption spectra—without further transformation. Relation (29) is indeed verified, where λ represents the wave length.

$$\int_{\omega_{qm}} \frac{\varepsilon_\omega}{\omega} \mathrm{d}\omega = \int_{\lambda_{qm}} \frac{\varepsilon_\lambda}{\lambda} \mathrm{d}\lambda \tag{29}$$

3.2 Set of isotropically diluted molecules

Gas phase absorption spectra of small molecules under low temperatures and pressures may fulfill most criteria corresponding to the previously mentioned hypothetic set of isotropically and homogeneously distributed akinetic and isolated molecules [21]. In such cases, it is indeed possible to study each absorption ray individually. Such a procedure is however, not usable for diluted molecules.

Indeed, let us now consider a single diluted molecular species. Each molecular entity of interest now exhibits, because of the influence of the solvent or of the matrix, many rovibrational degrees of freedom. As a consequence, each individual electronic transition is now associated to a huge density of rovibrational eigenstates and does no longer appear as a set of well separated rays but as a wide band. The integration of each individual rovibronic absorption ray is then no longer feasible and the corresponding molecular data can not be experimentally accessed anymore. As shown below, however, thanks to additional assumptions, different molecular data can be extracted.

First, the Born–Oppenheimer approximation[7] has to be used [17]. Each rovibronic eigenstate $|m\rangle$ is then assumed equal to the product of a rovibrational eigenstate $|m_{\mathrm{rot}}, m_{\mathrm{vib}}\rangle$ and an electronic eigenstate $|m_{\mathrm{elec}}\rangle$, as represented in equation (30).

$$|m\rangle = |m_{\mathrm{rot}}, m_{\mathrm{vib}}, m_{\mathrm{elec}}\rangle = |m_{\mathrm{rot}}, m_{\mathrm{vib}}\rangle\, |m_{\mathrm{elec}}\rangle \tag{30}$$

The electric dipole moment operator μ depends however, on all electronic *and* nuclear coordinates. As a consequence, the Born–Oppenheimer approximation is not sufficient in itself to allow the direct extraction of molecular data from electronic absorption spectra and the Franck–Condon approximation is then usually additionally used [17,21]. Within this framework, the transition dipole moment between two rovibronic eigenstates is assumed independent with respect to the rovibrational parts of the involved rovibronic eigenstates, which leads to relation (31).

$$\langle m|\, \mu\, |n\rangle = \mu_{m_{\mathrm{elec}} n_{\mathrm{elec}}}\, \langle m_{\mathrm{rot}}, m_{\mathrm{vib}}|\, n_{\mathrm{rot}}, n_{\mathrm{vib}}\rangle \tag{31}$$

[7] The justification of this approximation is too remote from the purpose of this article and is not discussed further here.

One of the most problematic point while investigating the electronic absorption bands of a diluted molecular species is that these bands very often overlap. Actually, isolated electronic absorption bands are rather rare. However, before treating more complex cases, let assume at the moment that we are here dealing with a well isolated absorption band resulting from an unique electronic transition between electronic states $|q_{\mathrm{elec}}\rangle$ and $|m_{\mathrm{elec}}\rangle$. In such a case, expressions (27) and (28) give rise to relations (32) and (33).

$$\int_{\mathrm{band}} \frac{\varepsilon_\omega}{\omega} \mathrm{d}\omega = \frac{N_A \pi}{3\hbar c \varepsilon_0 n_S \log_e(10)} \left(\frac{n_S^2+2}{3}\right)^2 \mu^2_{q_{\mathrm{elec}} m_{\mathrm{elec}}} \times \sum_{q_{\mathrm{rot}}, q_{\mathrm{vib}}} g_q \sum_{m_{\mathrm{rot}}, m_{\mathrm{vib}}} \langle q_{\mathrm{rot}}, q_{\mathrm{vib}}|\, m_{\mathrm{rot}}, m_{\mathrm{vib}}\rangle^2 \tag{32}$$

$$\int_{\mathrm{band}} \varepsilon_\omega d\omega = \frac{N_A \pi}{3\hbar c \varepsilon_0 n_S \log_e(10)} \left(\frac{n_S^2+2}{3}\right)^2 \mu^2_{q_{\mathrm{elec}} m_{\mathrm{elec}}} \times \sum_{q_{\mathrm{rot}}, q_{\mathrm{vib}}} g_q \sum_{m_{\mathrm{rot}}, m_{\mathrm{vib}}} \omega_{qm} \langle q_{\mathrm{rot}}, q_{\mathrm{vib}}|\, m_{\mathrm{rot}}, m_{\mathrm{vib}}\rangle^2 \tag{33}$$

In many every day life cases, electronic absorption spectra of diluted molecular species are measured at the thermodynamic equilibrium and at room or low temperature. It may then be assumed that all molecular entities of interest are in their electronic ground state or, at least, in a single electronic state $|q_{\mathrm{elec}}\rangle$, which leads to relation (34). This assumption is of course only valid if the life time of the electronic state of interest is much longer than the timescale of the experiment and if the energy differences between this electronic state of interest and the other electronic states of the system are much larger than $k_B T$, where k_B represents the Boltzmann constant and T the temperature. In other cases, statistical or time-dependent populations have to be considered for the different electronic states of the system, which leads to slightly more complete expressions that strongly depends on the exact experimental device. Therefore, such cases will not be considered further in this article.

$$\sum_{q_{\mathrm{rot}}, q_{\mathrm{vib}}} g_q = 1 \tag{34}$$

Thanks to relation (34) and on account of the closure relation (35), expression (32) can easily be simplified into (36).

$$\sum_{m_{\mathrm{vib}}} |m_{\mathrm{rot}}, m_{\mathrm{vib}}\rangle\, \langle m_{\mathrm{rot}}, m_{\mathrm{vib}}| = \mathbf{1} \tag{35}$$

$$\int_{\mathrm{band}} \frac{\varepsilon_\omega}{\omega} d\omega = \frac{N_A \pi}{3\hbar c \varepsilon_0 n_S \log_e(10)} \left(\frac{n_S^2+2}{3}\right)^2 \mu^2_{q_{\mathrm{elec}} m_{\mathrm{elec}}} \tag{36}$$

On the contrary, since ω_{qm} depends on m_{vib} and m_{rot}, relation (35) does not allow any further simplification of relation (33) and an additional approximation is then required: frequency ω_{qm} is assumed constant over the whole absorption band. The constant value which is most often chosen is that corresponding to the frequency $\omega_{\max}$ giving the largest contribution to the integral, i.e. the frequency for which ε_ω reaches a maximum. This approximation is of course valid only if the absorption band is tight enough and leads to relation (37).

$$\frac{1}{\omega_{\max}} \int_{\text{band}} \varepsilon_\omega \mathrm{d}\omega = \frac{N_A \pi}{3\hbar c \varepsilon_0 n_S \log_e(10)} \left(\frac{n_S^2+2}{3}\right)^2 \mu^2_{q_{\text{elec}} m_{\text{elec}}} \tag{37}$$

From a mathematical point of view, relation (37) is of course an approximation of relation (36), even if they are initially resulting from two different but mathematically exact integration methods and, as shown in the next sections, they can, in most cases, equally be used without further lost of precision.

4 One-dimensional harmonic oscillator

In this section is presented an academic and fully analytically solvable example whose purpose is to allow the quantification of the uncertainty introduced by the Franck–Condon approximation and of the divergence between relations (36) and (37).

A quantum system with two harmonic electronic states and a single nuclear coordinate, X, associated to a mass M, is considered. No rotation is involved in this example and the temperature is assumed null, which implies that the absorbent system is initially in the vibrational ground state of the electronic ground state. Both harmonic electronic states are assumed to be associated to the same vibrational frequency σ and arranged as pictured in Fig. 1. The value of interest is here assumed to be the so-called vertical transition dipole moment μ_{01} between both electronic states.

4.1 Franck–Condon approximation

The Franck–Condon approximation is here only tested on relation (32). A similar study performed on relation (33) would however, lead to the same conclusions. The electronic part of the transition electric dipole moment between both electronic states of the system is here assumed depending on X through relation (38), where K is a constant.

$$\mu_{\text{elec}} = \mu_0 (1 + KX) \tag{38}$$

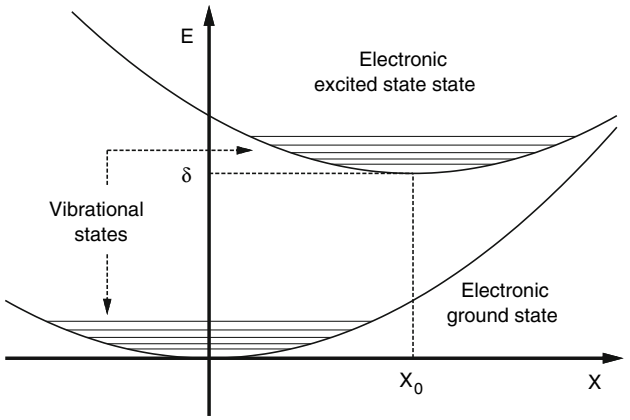

Fig. 1 Hypothetic one-dimensional system characterized by two harmonic electronic states, both associated to the vibrational frequency σ, and the single coordinate, X, associated to the mass M. Electronic energy minima are met at $X = 0$ ($E = 0$) and $X = X_0$ ($E = \delta$)

Considering this assumption and the previous ones, relation (32) has here to be replaced by relation (39).

$$\int_{\text{band}} \frac{\varepsilon_\omega}{\omega} \mathrm{d}\omega = \frac{N_A \pi}{3\hbar c \varepsilon_0 n_S \log_e(10)} \left(\frac{n_S^2+2}{3}\right)^2 \mu_0^2 \times \sum_{m_{\text{vib}}} \langle 0_{\text{vib}} | \, 1 + KX \, | m_{\text{vib}} \rangle^2 \tag{39}$$

Closure relation (35) then allows the replacement of the sum in the right-hand side member of relation (39) by $\langle 0_{\text{vib}} | \, (1 + KX)^2 \, | 0_{\text{vib}} \rangle$. The eigenstates of the harmonic oscillator are analytically well known [11]. Its ground state is, in particular, associated to wave function (40), which leads to relation (41).

$$0_{\text{vib}}(X) = \left(\frac{M\sigma}{\pi\hbar}\right)^{\frac{1}{4}} \exp\left(-\frac{M\sigma X^2}{2\hbar}\right) \tag{40}$$

$$\int_{\text{band}} \frac{\varepsilon_\omega}{\omega} \mathrm{d}\omega = \frac{N_A \pi}{3\hbar c \varepsilon_0 n_S \log_e(10)} \times \left(\frac{n_S^2+2}{3}\right)^2 \mu_0^2 \left(1 + \frac{K^2\hbar}{2M\sigma}\right) \tag{41}$$

This relation has to be compared with relation (36), which was obtained by applying the Franck–Condon approximation. It can be seen that, within the framework of this particular example, applying the Franck–Condon approximation would result in an overestimation of a factor $\sqrt{1 + K^2\hbar/(2M\sigma)}$ of the vertical transition electric dipole moment μ_0. It is remarkable that $\hbar/(2M\sigma)$ is equal to the average quadratic displacement of the harmonic oscillator over its ground state. From a numerical point of view, however, even a fluctuation of ±25% of μ_{elec} between $X = 0$ and $X = \pm\sqrt{\hbar/(2M\sigma)}$ leads to an overestimation of only 6% in the determination of the vertical transition electric dipole

moment μ_0, which is rather acceptable with respect to the other uncertainty sources, as shown within the next sections.

The divergence with and without the Franck–Condon approximation strongly depends on the molecular system of interest itself and no general rule can be drawn. From an experimental point of view, however, this kind of situation is only met in molecular systems that exhibit one or several floppy vibrational modes that strongly affect the electronic wave functions [14], or for spatially forbidden transitions that become observable in presence of vibronic couplings (cf. Sect. 5). In such cases, a more precise approach has to be considered like, for example, the Herzberg–Teller approximation [2,19,36]. In most other cases however, the Franck–Condon approximation is rather acceptable.

4.2 Integration methods

As previously mentioned, relation (37) is an approximation of relation (36). The purpose of this section is to provide an order of magnitude of this assumption by quantifying the divergence between these two expressions within the framework of the previously presented simple academic example. The Franck–Condon approximation is here assumed and the electronic part of the transition electric dipole moment is then now considered independent on X and equal to μ_0. Using then the fact that $\omega_{0,m}$ is equal to $\delta/\hbar + \sigma m_{\text{vib}}$, expressions (42) and (43) are derived from relations (33) and (32).

$$\int_{\text{band}} \frac{\varepsilon_\omega}{\omega} \mathrm{d}\omega = \frac{N_A \pi \mu_0^2}{3\hbar c \varepsilon_0 n_S \log_e(10)} \left(\frac{n_S^2+2}{3}\right)^2 \tag{42}$$

$$\frac{1}{\omega_{\max}} \int_{\text{band}} \varepsilon_\omega \mathrm{d}\omega = \frac{N_A \pi \mu_0^2}{3\hbar c \varepsilon_0 n_S \log_e(10)} \left(\frac{n_S^2+2}{3}\right)^2 \times \frac{\delta + \frac{1}{2} M\sigma^2 X_0^2}{\hbar \omega_{\max}} \tag{43}$$

Finally, since $\delta + M\sigma^2 X_0^2/$ is equal to the vertical transition energy ω_{vert}, i.e. the difference between the potential energy curves corresponding to both electronic states at the geometry of the energy minimum of the ground state, relation (44) is verified.

$$\frac{1}{\omega_{\max}} \int_{\text{band}} \varepsilon_\omega \mathrm{d}\omega = \frac{N_A \pi \mu_0^2}{3\hbar c \varepsilon_0 n_S \log_e(10)} \left(\frac{n_S^2+2}{3}\right)^2 \frac{\omega_{\text{vert}}}{\omega_{\max}} \tag{44}$$

It can then be seen that the error made by using the approximated expression (37) is here equal to $(\omega_{\text{vert}} - \omega_{\max}/\omega_{\max})$ and that both integration method are perfectly equivalent if ω_{vert} and $\omega_{\max}$ are equal. In real cases, however, $\omega_{\max}$ strongly depends on the way the rovibrational absorption bands are overlapping together and no general rule can here be drawn. Numerical values are provided within the next section. The previously mentioned error is however, generally negligible in both following cases, both being possibly simultaneously met:

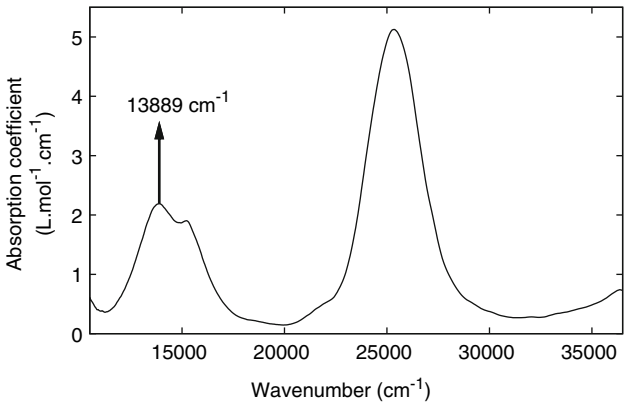

Fig. 2 UV–visible absorption spectrum of the $Ni(OH_2)_6^{2+}$ aqueous complex (see Appendix A for experimental details)

- $\delta \gg M\sigma^2 X_0^2/2$, where the vibrational correction is negligible with respect to ω_{vert}, which corresponds to tight absorption bands located at reasonably high absorption energies. An extreme illustration of this case is met in f-f transitions of lanthanides complexes [23].
- $M\sigma^2 X_0^2/2 \gg \hbar\sigma$, which corresponds to the classical limit of the harmonic oscillator, but which also corresponds to an absorption from low lying vibrational states of the electronic ground state to a high lying vibrational states of the electronic excited state.

For concluding, using the Franck–Condon approximation and/or the approximate relation (37) leads to the extraction of values stained with uncertainties. These last are however, rather small, especially if compared to the uncertainties resulting from the numerical integration itself, as shown in the next section.

5 UV–visible absorption spectrum of the $Ni(OH_2)_6^{2+}$ aqueous complex

Let now consider a realistic molecular entity, the $Ni(OH_2)_6^{2+}$ aqueous complex, and focus on its *d–d* electronic transitions. Since these lasts are spatially forbidden but spin-allowed, they give rise to absorption bands whose maxima correspond to absorption coefficients of a few L mol^{-1} cm^{-1}, as represented in Fig. 2. We will here only consider the complex band located around 14,000 cm^{-1}. Considering an O_h geometry for the $Ni(OH_2)_6^{2+}$ complex, this band corresponds to a $^3A_{2g} \rightarrow {}^3T_{1g}$ transition [8]. The exact origin of the complexity of this band is still under discussion and will then

not be investigated further in this article. We are here only concerned with the extraction of molecular data from this absorption band, considering that it is due to the single previously mentioned electronic transition. It has here however, to be emphasized that the fact that an absorption is observed whereas the corresponding transition is spatially forbidden most likely results from vibronic couplings inside the molecular entity. As a consequence, the data which is extracted from the absorption spectrum is not the vertical transition dipole moment, which is of course null since the transition is spatially forbidden, but an apparent electric transition dipole moment which depends on the values taken by the electronic part of the electric transition dipole moment for geometries close to the most likely one (cf. Sect. 4.1).

5.1 Integration technics

As previously mentioned, the numerical integration of absorption bands is a great source of error. Indeed, as can be seen in Fig. 2, the absorption coefficient does not decrease down to zero between the absorption band of interest and the neighboring ones. This essentially comes both from the overlapping of the electronic absorption bands and from the presence of noise in the spectrum. The question then rises of the method which has to be used for measuring the integral.

Many procedures exist for evaluating band integrals and all of them are, more or less, arbitrary. We present here four of them: the direct integral technic (noted D), the rapid gaussian technic (noted RG), the single gaussian fitting technic (noted SG) and the multiple gaussian fitting technic (noted MG). Here are their principles:

Technic D This technic first consists in arbitrary choosing a range of frequencies on which the absorption band of interest give a significant contribution. If no neighboring band is present and the absorption coefficient is decreasing down to zero, then the whole frequency range of the experimental spectrum is used. If no neighboring band is present, but the absorption coefficient is not decreasing down to zero, an arbitrary limit has to be chosen, otherwise, the integral diverges. Finally, if a neighboring band is present, the frequency corresponding to the minimum of absorption coefficient between the band of interest and its neighbor is used as a limit for the frequency range. The second step of the technic then consists in numerically integrating the absorption function (ε_ω or $\varepsilon_\omega/\omega$) over the chosen frequency range. Note that this technic is not so bad as it could first appear. Indeed, when two bands of almost equal intensities are overlapping, then, the missing part of the band of interest located outside the arbitrary chosen range of frequencies compensate with the contribution of the overlapping band located within the limits of this frequency range. This technic however, fails for overlapping bands of different intensities and for very noisy spectra.

Technic RG This technic consists in assuming that the absorption band of interest has a Gaussian shape described by the function $G_0 \exp\left[-(\omega-\omega_0)^2/\delta^2\right]$. G_0 is then equal to the maximum of the absorption function and the full width at half maximum (FWHM) Δ is equal to $2\delta\log_e(2)$. As a consequence, the integral of the absorption band is equal to $G_0\Delta\sqrt{\pi}/\log_e(4)$ ($\sqrt{\pi}/\log_e(4) \approx 1.279$). This technic is very simple but quite appealing. It is indeed rather rapid, since it does not require any explicit integral measurement, and takes advantage of compensation effects: if an absorption band is dissymmetric, what is lost on one side of the band by the gaussian approximation, is gain on the other side.

Technic SG The starting point of this method is identical to that of the RG method. The gaussian function is here however, explicitly fitted on the absorption band of interest. Note that this method does not necessarily gives better results than the RG method.

Technic MG Finally, for complex absorption bands, the fitting procedure may require the simultaneous usage of several gaussian functions. The methodology is then the following: a first function is fitted, and other additional functions are then sequentially introduced as long as the agreement between the experimental and the fitted functions is not sufficiently accurate, which means that the difference between the integrals obtained before and after adding the new function remains larger than the target precision.

The reason why gaussian functions are here used, even if absorption rays have lorentzian shapes (see relation (24) in Sect. 2.5), is due, first, to the gaussian shape of the wave function corresponding to the vibrational ground state in the harmonic oscillator approximation and, second, to the gaussian shape of the Boltzmann distribution which governs the population of the rovibrational states of the electronic ground state. Both tends indeed to give a pseudo-gaussian shape to electronic absorption bands of diluted molecules.

There is no good or bad method among those previously presented. Their quality indeed depends on the shape of the band of interest and on the target precision.

5.2 Extraction of molecular data

As can be seen on Fig. 2, ε_ω presents a maximum at $13{,}889\,\mathrm{cm}^{-1}$, whereas $\varepsilon_\omega/\omega$ presents a maximum at $13{,}793\,\mathrm{cm}^{-1}$ (not graphically represented). It can then be seen that both values are not exactly equal and differ by about 0.7%, which actually remains quite acceptable. Let us then chose $\omega_{\max}$ equal to $13{,}889\,\mathrm{cm}^{-1}$. On the basis of the approximations presented in the previous sections, this values should be equal to the vertical transition frequency ω_{vert}. One may however, hesitate while measuring $\omega_{\max}$ because the absorption function ε_ω exhibits two maxima whose intensities are rather similar at 13,889 and $15{,}209\,\mathrm{cm}^{-1}$. A possible

Table 1 Transition electric dipole moments extracted from the experimental absorption spectrum represented in Fig. 2 for the band located around 14,000 cm^{-1}

Reported values are obtained using integration technics D, RG, SG and MG, and by integrating $\varepsilon_\omega/\omega$ (relation (36)) or ε_ω (relation (37)). Technical details are reported in Appendix B

Integration technic	From $\varepsilon_\omega/\omega$ (10^{-2} D)	From ε_ω (10^{-2} D)	Absolute deviation	
			(10^{-2} D)	(%)
D	6.859	6.975	+0.116	+1.7
RG	7.397	7.457	+0.060	+0.8
SG	6.827	6.912	+0.085	+1.2
MG	6.727	6.828	+0.101	+1.5
Average value (10^{-2} D)	6.953	7.043		
Quadratic deviation (10^{-2} D)	0.261	0.245		
Quadratic deviation (%)	3.8	3.5		

solution would be to propose an intermediate value of $14{,}549 \pm 660^{-1}$, with then an uncertainty of about 5%. We will here however, strictly stick to the definition we gave for ω_{max} and keep the value of 13,889 cm^{-1}.

From the previous paragraph, it appears that even the experimental determination of the absorption energy, which first looks as a simple task, may give rise to significant uncertainties of several percents. We however, here voluntary chose a complex case and much precise values are usually obtained. The same conclusion can however, unfortunately not be drawn for the determination of the transition electric dipole moment, as shown below.

In Table 1 are reported the values obtained using the different integration technics previously presented and both integration methods depicted by relations (36) and (37). Technical details are reported in Appendix B.

Values reported in the fourth and fifth columns, confirm the quite small character of the deviation between both integration methods (36) and (37). Indeed, whatever the integration technic, both values obtained using these methods only differ by about 1%. Only the D technic gives rise to a slightly higher deviation (1.7%), but this simply results from the quite large frequency range used in that case, which makes the deviation between $\varepsilon_\omega/\omega$ and $\varepsilon_\omega/\omega_{max}$ more sensitive. This does however not change the fact that the deviation resulting from the choice of the integration method remains much lower than that resulting from the choice of the integration technics (3.5 and 3.7%, respectively).

If these last uncertainties are larger than those previously mentioned, they however, remain quite reasonable considering the complexity of the absorption band and the raw character of some of the technics used, like D and RG in particular. This result may appear surprising, but it must not be forgotten that we are here dealing with integrals, and some variations of the absorption function may look rather large but have few effects on the integrated area located under the curve representing the function.

In this particular case, the RG technic is apparently giving the worst result, since other three values only deviate by 0.8 and 0.9% respectively for both integration methods. This is however, not a general result. The previously presented integration technics do indeed not have intrinsic qualities. The relevance of their numeric results strongly depend on the shape of the absorption function. We then strongly suggest that, while extracting molecular data from absorption bands, several integration technics are used and compared, the deviation between them being used as a confidence criterium.

6 Conclusion

In this article, we performed a clear sequential derivation of the relations leading from microscopic molecular theoretically accessible data to macroscopic experimentally accessible data within the framework of UV–visible absorption spectra of optically linear molecular entities homogeneously and isotropically diluted in transparent homogeneous and isotropic matrices or solvents. At each step of the derivation, the assumptions used and their limitations have been emphasized. The return sequence allowing the extraction of molecular data from UV–visible absorption spectra of diluted molecules have then also been derived and illustrated using two examples: an academic one and an experimental one.

It has then been shown that, for extracting electronic molecular data, both the Born-Oppenheimer and the Franck–Condon approximation are generally required, which makes it only possible to extract apparent transition electric dipole moments and transition energies which might be slightly different from the values accessible by other means like theory or gas phase measurements.

From a numerical point of view, it has also been shown that using any of both integration methods (36) or (37) does not make so much difference, and that the greatest uncertainties results from integration technics. Note that the highest deviation we here obtained between the integration technics we used is only of 3.7% but this becomes much worse when absorption bands are strongly overlapping.

Finally, from a more general point of view, the same approximations and methodology can be used for extracting molecular data from multiphoton absorption spectra, as it has already been shown, for example, within the framework of two-photon absorption [13].

Appendix A: experimental details

Preparation of the $Ni(OH_2)_6^{2+}$ solution The solution was prepared by dissolving 205.2 ± 0.2 mg of solid $NiSO_4$ ($NiSO_4 \cdot 6H_2O$, 262.83 ± 0.01 g mol^{-1}) in water up to reach 50.00 ± 0.05 mL. The dissolution reaction is complete (the maximum solubility of $NiSO_4$ in water is such that it can represent up to 27.55% of the weight of the solution at 298 K [6]) and all Ni^{2+} ions are then involved in $Ni(OH_2)_6^{2+}$ complexes. The concentration of the solution is then equal to $(1.561 \pm 0.002) \times 10^{-2}$ mol L^{-1}.

UV–vis absorption spectrum measurement Spectra was measured thanks to a JASCO VIS–UV V-550 spectrophotometer [22] whose uncertainty is 0.15% concerning the absorbance and 1 nm concerning the wavelength, using a 10.00 ± 0.01 mm thick HELMA QS-10 Suprasil® quartz cell whose refraction index is uniform between 250 and 2,000 nm and equal to 1.458 at 20°C [16]. The uncertainty related to the absorption spectrum is then equal to 0.4% concerning the absorption coefficient and to 0.3% concerning the wave number.

Appendix B: integration details

In this section are gathered the details concerning the integration of the absorption band exhibited by aqueous Ni^{+2} ions around 14,000 cm^{-1}. Refractive index of the solvent (water): 1.33283 at 20 °C [1].

Technic D Frequency range: 10,870–19,920 cm^{-1} for ε_ω and 10,881–20,000 cm^{-1} for $\varepsilon_\omega/\omega$.

Technic RG FWHM: 3,571 cm^{-1} for ε_ω and 3,500 cm^{-1} for $\varepsilon_\omega/\omega$. Maxima: 0.2189 m^2 mol^{-1} at 13,889 cm^{-1} for ε_ω and 1.5824×10^{-7} m^3 mol^{-1} at 13,793 cm^{-1} for $\varepsilon_\omega/\omega$.

Technic SG $G_0 = 0.2144$ m^2 mol^{-1}, $\omega_0 = 14{,}354$ cm^{-1}, and $\delta = 2{,}261$ cm^{-1} for ε_ω. $G_0 = 1.5091 \times 10^{-7}$ m^3 mol^{-1}, $\omega_0 = 14{,}172$ cm^{-1}, and $\delta = 2{,}255$ cm^{-1} for $\varepsilon_\omega/\omega$. Frequency range used for the fitting procedure: see D technic above.

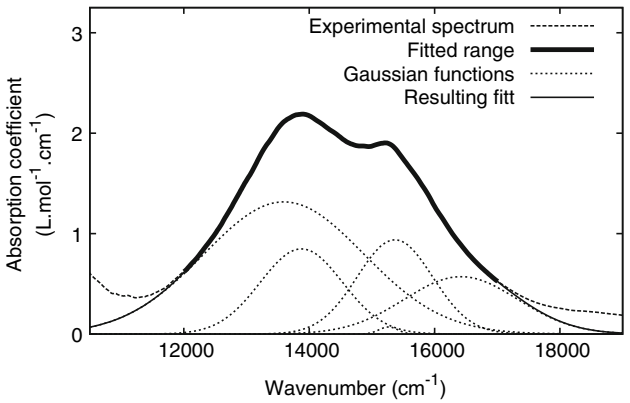

Fig. 3 Adsorption band located around 14,000 cm^{-1} (*dashed line*) partially (*thick solid line*) fitted thanks to 5 gaussian functions (*dotted lines*)

Table 2 Fitted parameters for the MG technic

Function	G_0 (m^2 mol^{-1})	ω_0 (cm^{-1})	δ (cm^{-1})
For ε_ω			
1	0.17197	14,210	2, 149.5
2	−0.33134	14,685	946.7
3	0.07167	15,265	202.2
4	0.92397	15,299	1, 333.7
5	−0.69581	15,577	1, 174.1
Function	G_0 (10^{-7} m^3 mol^{-1})	ω_0 (cm^{-1})	δ (cm^{-1})
For $\varepsilon_\omega/\omega$			
1	0.95591	13,455	1, 804.9
2	0.63062	13,848	937.5
3	0.04745	15,261	204.9
4	0.59310	15,339	842.7
5	0.36309	16,311	1, 318.8

Technic MG Five gaussian functions have here been used, as represented in Fig. 3 for ε_ω (the corresponding figure but for $\varepsilon_\omega/\omega$ is very similar and then not represented). The frequency range used for the fitting procedure has been restricted to 12,000–17,000 cm^{-1}. The corresponding parameters are gathered in Table 2.

References

1. Weast RC (1979) Handbook of Chemistry, 60th edn. CRC Press, Boca Raton
2. Albrecht AC (1960) "forbidden" character in allowed electronic transitions. J Chem Phys 33(1):156–169
3. Andrews L, Moskovits L (1989) Chemistry and physics of matrix isolated species. NorthHolland, Amsterdam

4. Atkins PW, Friedman RS (2001) Molecular quantum mechanics, 3rd edn. Oxford University Press, New York
5. Bell JE (1981) Spectroscopy in biochemistry, vol 1, 2. CRC Press, Boca Raton
6. Blachnik R (1998) Elemente, anorganische Verbindungen und Materialen, Minerale, Taschenbuch für Chemiker und Physiker, vol 3, 4th edn. Springer, Berlin
7. Condon EU, Shortley GH (1991) The theory of atomic spectra. Cambridge University Press, Cambridge
8. Cotton AF, Wilkinson G, Murillo CA, Bochmann M (1999) Advanced inorganic chemistry, 6th edn. Wiley, New York
9. Debye PJW (1929) Polar molecules. Dover, New York
10. Delgass WN, Haller GL, Kellerman R, Lunsford JH (1979) Spectroscopy in heterogenous catalysis. Academic Press, New York
11. Dodd RE (1962) Chemical spectroscopy. Elsevier Student, Amsterdam
12. Feynman RP, Leighton RB, Sands M (2005) Feynman lectures on physics, definitive and expanded edition, 2nd edn. Addison Wesley, Redwood City
13. Fortrie R, Chermette H (2006) Two-photon absorption strength: anew tool for the quantification of two-photon absorption. J Chem Phys 124:204104
14. Fortrie R, Chermette H (2007) Vibronic quasi-free rotation effects in biphenyl-like molecules. TD-DFT study of bifluorene. J Chem Theor Comput 3(3):852–859
15. Fortrie R, Anémian R, Stephan O, Mulatier JC, Baldeck PL, Andraud C, Chermette H (2007) Enhancement of two-photon absorption via oligomerization. a route for the engineering of two-photon absorbers in the visible range. J Phys Chem C 111(5): 2270–2279
16. http://www.hellmafrance.fr
17. Harris DC, Bertolucci MD (1989) Symmetry and spectroscopy. An introduction to vibrational and electronic spectroscopy. Dover Publications, New York
18. Heisenberg W (1925) Z Phys 33:879
19. Herzberg G, Teller E (1933) Vibrational structure of electronic transitions for polyatomic molecules. Z Physik Chem B 21:410–446
20. Hollas JM (1982) High resolution spectroscopy. Butterworths, London
21. Hollas JM (2000) Modern spectroscopy, 4th edn. Wiley, Chichester
22. http://www.jascofrance.fr
23. Huheey JE, Keiter EA, Keiter RL (1997) Inorganic chemistry: principles of structure and reactivity, 4th edn. HarperCollins, New York
24. Klöpffer W (1984) Introduction to polymer spectroscopy, polymers/properties and applications, vol 7. Springer, Berlin
25. Kuhn W (1925) Z Phys 33:408
26. Kuzmany H (1998) Solid-state spectroscopy and its applications. Springer, Berlin
27. Leach AR, Gillet V (2003) An introduction to chemoinformatics. Kluwer Academic, Dordrecht
28. Lorentz HA (1951) The theory of electrons and its applications to the phenomena of light and radiant Heat. In: Teubner B.G. (ed) Leipzig, 1916. Dover, New York
29. Maier JP (1989) Ion and cluster ion spectroscopy. Elsevier, Amsterdam
30. McNaught AD, Wilkinson A (1997) IUPAC compemdium of chemical terminology. The gold book, 2nd edn. Blackwell Science, Oxford
31. Nakamoto K, McCarthy PJ (1968) Spectroscopy and structrure of metal chelate compounds. Wiley, New York
32. Onsager L (1936) Electric moments of molecules in liquids. J Am Chem Soc 58(8):1486–1493
33. Orr BJ, Ward JF (1971) Perturbation theory of the non-linear optical polarization of an isolated system. Molec Phys 20:513–526
34. Perkampus HH (ed) (1995) Encyclopedia of spectroscopy. VCH, Weinheim
35. Reiche F, Thomas W (1925) Z Phys 34:510
36. Roche M, Jaffé HH (1974) A modification of the Herzberg-Teller expension for vibronic coupling. J Chem Phys 60(4):1193–1196
37. Sierka M, Sauer J (2000) Finding transition structures in extended systems: a strategy based on a combined quantum mechanics-empirical valence bond approach. J Chem Phys 112(16):6983–6996
38. Spezia R, Duvail M, Vitorge P, Cartailler T, Tortajada J, Chillemi G, D'Angelo P, Gaigeot MP (2006) A coupled Car-Parrinello molecular dynamics and EXAFS data analysis investigation of aqueous co^{2+}. J Phys Chem A 110(48):13081–13088
39. Thomas W (1925) Naturwiss 13:627
40. Vollhardt KPC, Shore NE (1994) Organic chemistry. 2nd edn. Freeman, New York
41. Williams DH, Fleming I (1995) Spectroscopic methods in organic chemistry, 5th edn. McGraw Hill, London